arXiv:cond-mat/0208245v1 [cond-mat.stat-mech] 13 Aug 2002

Spin-Wave Description of Nuclear Spin-Lattice Relaxation in $Mn_{12}O_{12}$ Acetate

Shoji Yamamoto and Takashi Nakanishi
Division of Physics, Hokkaido University, Sapporo 060-0810, Japan
(16 May 2002)

In response to recent nuclear-magnetic-resonance (NMR) measurements on the molecular cluster $Mn_{12}O_{12}$ acetate, we study the nuclear spin-lattice relaxation rate $1/T_1$ developing a modified spin-wave theory. Our microscopic new approach, which is distinct from previous macroscopic treatments of the cluster as a rigid spin of $S = 10$, not only excellently interprets the observed temperature and applied-field dependences of $1/T_1$ for ^{55}Mn nuclei but also strongly supports the ^{13}C NMR evidence for spin delocalization over the entire molecule.

PACS numbers: 76.50.+g, 05.30.Jp, 75.50.Xx

Mesoscopic magnetism [1] is one of the hot topics in materials science, where we can observe a quantum-to-classical crossover on the way from molecular to bulk magnets. Metal-ion magnetic clusters are thus interesting and among others is $[Mn_{12}O_{12}(CH_3COO)_{16}(H_2O)_4]$ [2] (hereafter abbreviated as Mn12), for which quantum tunneling of the magnetization [3,4] was observed for the first time. There are three symmetry-inequivalent Mn sites in the Mn12 cluster (see Fig. 1). The four inner Mn^{4+} spins and the eight outer Mn^{3+} spins are directed antiparallel to each other and exhibit a novel ground state of total spin $S = 10$ [5]. Resonant magnetization tunneling in such high-spin molecules can be an evidence for the validity of quantum mechanical approaches at the nanometer scale.

The simplest Hamiltonian for the Mn12 cluster in a field may be given by $\mathcal{H} = -D(S^z)^2 - g\mu_{\rm B}\boldsymbol{S}\cdot\boldsymbol{H}$, where the molecular cluster is strictly treated as a rigid $S = 10$ object with single-axis magnetic anisotropy. While such a macroscopic treatment of the molecule interprets well quantum relaxation of the magnetization [6,7], recent electron-paramagnetic-resonance (EPR) measurements [8] suggest a possible breakdown of the spin-10 description. Although a microscopic treatment of each Mn moment is necessary for further understanding of nanoscale magnets and is interesting in itself, the total spin states in the Mn12 cluster is too large even for modern computers to directly handle. Thus it is an idea [9] that the Mn^{3+}-Mn^{4+} pairs connected by the strongest exchange interaction J_1 construct composite spins $\frac{1}{2}$. This eight-spin scheme explains well the magnetization [3,10], inelastic-neutron-scattering [11,12], and EPR [12,13] measurements at sufficiently low temperatures. However, a recent skillful numerical-diagonalization study [14] has shown that even the ground state is quite sensitive to the less dominant exchange interactions J_2, J_3, and J_4 as well, throwing doubt on a parameter assignment within the eight-spin scheme [9], $J_1 \sim -150\,{\rm cm}^{-1}$, $J_2 \simeq J_3 \sim -60\,{\rm cm}^{-1}$, and $J_4 \sim 0$.

It is also unfortunate for this eight-spin model to be less applicable to nuclear-magnetic-resonance (NMR) measurements, which have vigorously been carried out for the Mn12 cluster [15–20] in recent years. Although the nuclear spin-lattice relaxation time T_1 can serve as a probe to the electron spin dynamics within the molecule, it is not yet interpreted beyond the spin-10 description. The early NMR studies on the Mn12 cluster were performed by using proton [15,17] or deuteron [16] nuclei as probes and therefore the interpretation was plagued by the averaging effect over the numerous protons and the weakness of the hyperfine coupling to the Mn moments. In order to obtain more direct information on the local magnetic properties, ^{55}Mn NMR measurements [18,19] have recently been performed. There has also appeared an elaborate ^{13}C NMR evidence [20] of the paramagnetic spin density of the cluster being delocalized over the entire molecule. Now we make our first attempt to interpret microscopically the nuclear spin-lattice relaxation-time measurements, developing a modified spin-wave theory [21].

We introduce a microscopic Hamiltonian for the Mn12 cluster as

$$\mathcal{H} = -\sum_{l=1}^{N}\Big[2J_1\boldsymbol{s}_l\cdot\boldsymbol{S}_l + 2J_2(\boldsymbol{s}_l\cdot\widetilde{\boldsymbol{S}}_l + \widetilde{\boldsymbol{S}}_l\cdot\boldsymbol{s}_{l+1}) + 2J_3(\boldsymbol{s}_l\cdot\boldsymbol{s}_{l+1} + \frac{1}{2}\boldsymbol{s}_l\cdot\boldsymbol{s}_{l+2}) + 2J_4(\boldsymbol{S}_l\cdot\widetilde{\boldsymbol{S}}_l + \widetilde{\boldsymbol{S}}_l\cdot\boldsymbol{S}_{l+1}) + D_2(S_l^z)^2 + D_3(\widetilde{S}_l^z)^2 + g\mu_{\rm B}H(s_l^z + S_l^z + \widetilde{S}_l^z)\Big], \qquad (1)$$

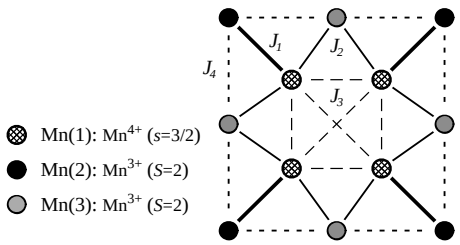

FIG. 1. Schematic plot of the Mn12 cluster. Inequivalent sites Mn(1), Mn(2), and Mn(3) are occupied by Mn^{4+} ions with $s = \frac{3}{2}$, Mn^{3+} ions with $S = 2$, and Mn^{3+} ions with $S = 2$, respectively. There exist four types of exchange interaction between them: J_1, J_2, J_3, and J_4, which are drawn by thick solid, dashed, thin solid, and dotted lines, respectively.

where $\boldsymbol{s}_l$, $\boldsymbol{S}_l$, and $\widetilde{\boldsymbol{S}}_l$ are the spin operators for the Mn(1) (spin $\frac{3}{2} \equiv s$), Mn(2) (spin $2 \equiv S$), and Mn(3) (spin $2 \equiv S$) sites in the lth unit, and N, the number of the elementary units, is equal to 4. The strongest exchange interaction J_1 and the next leading antiferromagnetic interaction J_2 were reliably estimated at $-150\,\mathrm{cm}^{-1}$ and $-60\,\mathrm{cm}^{-1}$, respectively, but the rest of the parameters remain to be fixed. Taking account of previous investigations, we adopt two contrasting parameter sets: (a) $J_1 = -150\,\mathrm{cm}^{-1}$, $J_2 = -60\,\mathrm{cm}^{-1}$, $J_3 = 60\,\mathrm{cm}^{-1}$, $J_4 = 30\,\mathrm{cm}^{-1}$ [10,22]; (b) $J_1 = -150\,\mathrm{cm}^{-1}$, $J_2 = -60\,\mathrm{cm}^{-1}$, $J_3 = -30\,\mathrm{cm}^{-1}$, $J_4 = 30\,\mathrm{cm}^{-1}$ [9,14]. As for the anisotropy parameters, there is much less information. When the molecule is treated as a rigid spin-10 object, the macroscopic uniaxial crystalline anisotropy parameter D is determined so as to fit the zero-field separation between the $M = \pm 10$ and $M = \pm 9$ levels, which is about 14 K [5,9]. Hence it is natural to choose the local single-ion anisotropy parameters, which describe the Jahn-Teller-distorted Mn^{3+} ions [23], within the same scheme [12]. Setting D_2 and D_3 both equal to $1.5\,\mathrm{cm}^{-1}$, we obtain the excitation energy of 13.7 K in the following spin-wave treatment. The g factors are all set equal to 2 [19].

We consider a spin-wave treatment of the Hamiltonian (1) introducing the bosonic operators for the spin deviation in each sublattice via $s_l^z = -s + a_{l,1}^\dagger a_{l,1}$, $s_l^+ = \sqrt{2s}\, a_{l,1}^\dagger$; $S_l^z = S - a_{l,2}^\dagger a_{l,2}$, $S_l^+ = \sqrt{2S}\, a_{l,2}$; $\widetilde{S}_l^z = S - a_{l,3}^\dagger a_{l,3}$, $\widetilde{S}_l^+ = \sqrt{2S}\, a_{l,3}$. We carry out the Bogoliubov transformation in the momentum space,

$$\begin{aligned} a_{k,1} &= -\psi_{11}(k)\, b_{k,1}^\dagger - \psi_{12}(k)\, b_{k,2}^\dagger + \psi_{13}(k)\, b_{k,3}\,, \\ a_{k,2} &= \psi_{21}^*(k)\, b_{k,1} + \psi_{22}^*(k)\, b_{k,2} - \psi_{23}^*(k)\, b_{k,3}^\dagger\,, \\ a_{k,3} &= \psi_{31}^*(k)\, b_{k,1} + \psi_{32}^*(k)\, b_{k,2} - \psi_{33}^*(k)\, b_{k,3}^\dagger\,, \end{aligned} \tag{2}$$

so as to reach the diagonal Hamiltonian

$$\mathcal{H} = E_{\mathrm{g}} + \sum_k \sum_{j=1,2,3} \omega_j(k)\, b_{k,j}^\dagger b_{k,j}\,, \tag{3}$$

where $E_{\mathrm{g}} = 8Ss(J_1 + 2J_2) - 12s^2 J_3 - 16S^2 J_4 - 4S^2(D_2 + D_3) - g\mu_{\mathrm{B}} H(2S - s)$. The numerically calculated dispersion relations $\omega_i(k)$ for the two parameter sets are shown in Fig. 2. The lowest-lying ferromagnetic ($\circ$) and the antiferromagnetic ($\times$) branches are both sensitive to J_3, while the second ferromagnetic ($\diamond$) branch exhibits little dependence on J_3.

The core idea of the so-called modified spin-wave theory is summarized as constructing reliable thermodynamics in low dimensions by controlling the boson number. Constraining the total magnetization to be zero, Takahashi [24] obtained an excellent description of the low-temperature thermodynamics of one-dimensional Heisenberg ferromagnets. His idea that the thermal spin deviation, that is, the number of thermally induced bosons, should be equal to the ground-state magnetization may be replaced by [21]

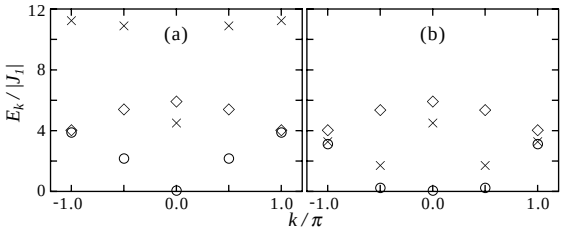

FIG. 2. Dispersion relations of the ferromagnetic ($\circ, \diamond$) and antiferromagnetic ($\times$) spin waves, which lie in the subspace of $M = 9$ and that of $M = 11$, respectively, for the parameter sets (a) and (b).

$$\sum_k \sum_{j=1,2,3} \bar{n}_{k,j} \sum_{i=1,2,3} |\psi_{ij}(k)|^2 = 8S + 4s\,, \tag{4}$$

for the ferrimagnetic Mn12 cluster, where $\bar{n}_{k,j}$ is expressed as $\sum_{n_1,n_2,n_3=0}^{\infty} n_j P_k(n_1, n_2, n_3)$ with P_k being the probability of n_j spin waves of mode-j appearing in the k-momentum state. Equation (4) claims that the thermal fluctuation should cancel the *staggered* magnetization instead of the *uniform* one, in response to the present ferrimagnetic ground state. Minimizing the free energy $F = E_{\mathrm{g}} + \sum_k \sum_{j=1,2,3} \bar{n}_{k,j}\omega_j(k) + k_{\mathrm{B}}T \sum_k \sum_{n_1,n_2,n_3} P_k(n_1, n_2, n_3) \ln P_k(n_1, n_2, n_3)$ with respect to P_k at each k under the condition (4) together with the trivial constraints $\sum_{n_1,n_2,n_3} P_k(n_1, n_2, n_3) = 1$, we obtain the optimum distribution functions as

$$\bar{n}_{k,j} = \frac{1}{\mathrm{e}^{[\omega_j(k) + \mu \sum_{i=1,2,3} |\psi_{ij}(k)|^2]/k_{\mathrm{B}}T} - 1}\,, \tag{5}$$

where μ is a Lagrange multiplier due to Eq. (4). Once the distribution is determined, we can readily calculate any thermal quantities such as the internal energy $U = E_{\mathrm{g}} + \sum_k \sum_{j=1,2,3} \bar{n}_{k,j}\omega_j(k)$ and the magnetic susceptibility $\chi = [(g\mu_{\mathrm{B}})^2/k_{\mathrm{B}}T] \sum_{j=1,2,3} \bar{n}_{k,j}(1 + \bar{n}_{k,j})$.

Although the above-demonstrated modified spin-wave scheme of the ferrimagnetic version generally works well in low dimensions [25,26], it is not yet applicable to the Mn12 cluster as it is. Due to the significant Jahn-Teller distortion, the lowest excited states of $M = \pm 9$ are separated from the ground states of $M = \pm 10$ by a finite energy Δ, which is incompatible with the condition (4). In isotropic ferrimagnets, there exists a zero-energy excitation and therefore a certain number of bosons naturally survive at low temperatures. The grandcanonical constraint (4) not only works so as to suppress the thermal divergence of the boson number at high temperatures but also gives a precise description of the low-temperature thermodynamics [25]. On the other hand, once a gap Δ opens, the boson number should exponentially decreases as $\propto \mathrm{e}^{-\Delta/k_{\mathrm{B}}T}$ at low temperatures, while the constraint (4) still keeps it finite even at $T \to 0$. In order to eliminate the shortcoming, we replace Eq. (4) by

$$\sum_k \sum_{j=1,2,3} \bar{n}_{k,j} \sum_{i=1,2,3} |\psi_{ij}(k)|^2 = (8S + 4s)\, \mathrm{e}^{-\Delta/k_{\mathrm{B}}T}\,. \tag{6}$$

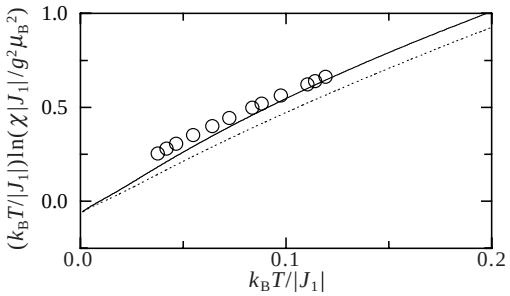

FIG. 3. Temperature dependences of the zero-field magnetic susceptibility for the parameter sets (a) (dotted line) and (b) (solid line). Experimental observations [5,9] (○) are also shown for reference, where we have assumed that $g = 2$ [13].

This is quite natural modification of the theory, because the new constraint (6) remains the same as the authorized one (4) except for the sufficiently low-temperature region $k_BT \lesssim \Delta$. It is also convincing that Eq. (6) smoothly turns into Eq. (4) as $\Delta \to 0$. In fact, the thus-calculated susceptibility looks reasonable in every aspect. In Fig. 3, we make a logarithmic plot of the zero-field susceptibility as a function of T in order to elucidate its low-temperature behavior. Regardless of parametrization, χ exhibits an initial exponential behavior $\propto \mathrm{e}^{-\Delta/k_BT}$ with $\Delta \simeq 13.7\,\mathrm{K}$. The calculations are further consistent with the experimental findings [5,9], implying that the parameter set (b) may better describe the Mn12 cluster.

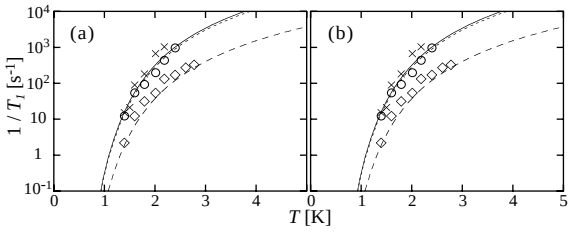

FIG. 4. Semilog plots of $1/T_1^{(i)}$ as a function of T under no external field for the parameter sets (a) and (b). The calculations, dashed [Mn(1)], dotted [Mn(2)], and solid [Mn(3)] lines, are compared with experiments [19], ⋄ [Mn(1)], ○ [Mn(2)], and × [Mn(3)].

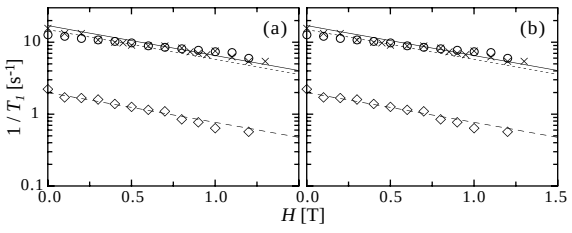

FIG. 5. Semilog plots of $1/T_1^{(i)}$ as a function of H at $T = 1.4\,\mathrm{K}$ for the parameter sets (a) and (b). The calculations, dashed [Mn(1)], dotted [Mn(2)], and solid [Mn(3)] lines, are compared with experiments [19], ⋄ [Mn(1)], ○ [Mn(2)], and × [Mn(3)].

Considering the electronic-nuclear energy-conservation requirement, the Raman process should play a leading role in the nuclear spin-lattice relaxation. The large zero-field energy splitting, which is associated with the single-ion anisotropy, not only makes the direct process irrelevant but also reduces the possibility of an odd-number-of-magnon process being realized. The Raman relaxation rate for the $^{55}\mathrm{Mn}(i)$ nucleus is given by

$$\frac{1}{T_1^{(i)}} = \frac{4\pi\hbar(g\mu_B\gamma_N)^2}{\sum_n \mathrm{e}^{-E_n/k_BT}} \sum_{n,m} \mathrm{e}^{-E_n/k_BT} \times \left|\langle m|A_i\sigma_{l,i}^z|n\rangle\right|^2 \delta(E_m - E_n - \hbar\omega_N)\,, \tag{7}$$

where $\sigma_{l,i}^z = s_l^z, S_l^z, \widetilde{S}_l^z$ for $i = 1, 2, 3$, respectively, A_i is the dipolar coupling constant between the nuclear and electronic spins on the $\mathrm{Mn}(i)$ site, $\omega_N \equiv \gamma_N H$ is the Larmor frequency of the nucleus with γ_N being the gyromagnetic ratio, and the summation $\sum_n$ is taken over all the electronic eigenstates $|n\rangle$ with energy E_n. Taking account of the significant difference between the electronic and nuclear energy scales ($\hbar\omega_N \lesssim 10^{-5}J$), the relaxation rate (7) is expressed in terms of the spin waves as

$$\frac{1}{T_1^{(i)}} = \frac{2\hbar(g\mu_B\gamma_N A_i)^2}{N} \sum_{j=1,2,3} \sum_{\{k,k'\}} |\Delta\omega_j(k)|^{-1} \times |\psi_{ij}(k)|^2 |\psi_{ij}(k')|^2 \bar{n}_{k,j}(\bar{n}_{k',j} + 1)\,, \tag{8}$$

where $\sum_{\{k,k'\}}$ denotes the limited summation of (k, k') over $(-\pi, -\pi)$, $(-\frac{\pi}{2}, -\frac{\pi}{2})$, $(0, 0)$, $(\frac{\pi}{2}, \frac{\pi}{2})$, $(\frac{\pi}{2}, -\frac{\pi}{2})$, and $(-\frac{\pi}{2}, \frac{\pi}{2})$, and $\Delta\omega_j(k) = [\omega_j(k + 2\pi/N) - \omega_j(k)]/(2\pi/N)$.

We show the thus-calculated $1/T_1^{(i)}$ as functions of T (Fig. 4) and H (Fig. 5) in comparison with the measurements [19], where the coupling constants A_i are the only adjustable parameters in reproducing both the T- and H-dependences and have been chosen as Table I. Though the calculations (a) and (b) look similar, Table I clearly shows that the parameter assignment (b) much more reasonably describes the Mn12 cluster. In response to asking whether the exchange interaction J_3 is ferromagnetic [10,22] or antiferromagnetic [9,14], we definitely answer that it is antiferromagnetic. Furthermore, we are skeptical of neglecting J_4 [9,10], for which the $S = 10$ ground state is much less stable [14] and the coupling constants are significantly underestimated in our calculation.

The observed temperature dependence of $1/T_1^{(i)}$, which is the same for $i = 1, 2, 3$, suggests that the spin dynamics of the local Mn moments is completely correlated. All the observations can indeed be interpreted within the Raman relaxation process. In the momentum summation in Eq. (8), the contribution from $(j; k, k') = (1; 0, 0)$ $(S = 10, M = 9)$ is predominant, while those from $(j; |k|, |k'|) = (1, \frac{\pi}{2}, \frac{\pi}{2})$ $(S = 9, M = 9)$ at most amount to a few percent of the total at $T = 1.4\,\mathrm{K}$. The spin dynamics is thus confined within fluctuations of the total spin moment $S = 10$ of the ground state at suffi-

ciently low temperatures. Although such a picture is intuitively convincing, we have to pay attention to a recent experimental report [27] that the hyperfine field of the Mn^{3+} ion is in fact anisotropic and exhibits a predominant dipolar contribution, whereas that of the Mn^{4+} ion is isotropic and originates from the Fermi contact. In this context, it is interesting to compare carefully the theoretical ($A_i^{\rm th}$) and experimental ($A_i^{\rm ex}$) findings for the coupling constants. Assuming the set (b), $A_1^{\rm th} \simeq 2.4 A_1^{\rm ex}$, $A_2^{\rm th} \simeq 1.7 A_2^{\rm ex}$, and $A_3^{\rm th} \simeq 1.2 A_3^{\rm ex}$. Somewhat larger deviation of the theory from the experiment for A_1 implies that the nuclear spin-lattice relaxation on the Mn(1) site may not primarily be Raman active but be strongly influenced by the surrounding Mn^{3+} ions.

The slight difference between the field dependences of $1/T_1^{(2)}$ and $1/T_1^{(3)}$ can not be elucidated within the present calculation, but this is probably due to the equal treatment of the Mn(2) and Mn(3) sites, $g_2 = g_3$ and $D_2 = D_3$. Considering that experimental analyses [18,19] have not yet entered into such details, our first step toward the microscopic description of the Mn12 cluster is really successful. We stress that the success of our spin-wave description contributes in itself toward verifying the recently reported intramolecular spin delocalization [20]. Our theory promises future investigations into various molecular magnets over the static, dynamic, quantum, and thermal properties.

The authors are grateful to Prof. T. Goto for fruitful discussion. This work was supported by the Japanese Ministry of Education, Science, and Culture and by the Sumitomo Foundation.

[1] D. Gatteschi, A. Caneschi, L. Pardi, and R. Sessoli, Science **265**, 1054 (1994).
[2] T. Lis, Acta Crystallogr. Sect. B **36**, 2042 (1980).
[3] J. R. Friedman, M. P. Sarachik, J. Tejada, and R. Ziolo, Phys. Rev. Lett. **76**, 3830 (1996).
[4] L. Thomas, F. Lionti, R. Ballou, D. Gatteschi, R. Sessoli, and B. Barbara, Nature (London) **383**, 145 (1996).
[5] A. Caneschi, D. Gatteschi, R. R. Sessoli, A. L. Barra, L. C. Brunel, and M. Guillot, J. Am. Chem. Soc. **113**, 5873 (1991).
[6] N. V. Prokof'ev adn P. C. E. Stamp, Phys. Rev. Lett. **80**, 5794 (1998).
[7] S. Miyashita, K. Saito, H. Kobayashi, and H. De Raedt, J. Phys. Soc. Jpn. **69**, Suppl. A, 395 (2000).
[8] S. Hill, J. A. A. J. Perenboom, N. S. Dalal, T. Hathaway, T. Stalcup, and J. S. Brooks, Phys. Rev. Lett. **80**, 2453 (1998).
[9] R. Sessoli, H.-L. Tsai, A. R. Schake, S. Wang, J. B. Vincent, K. Folting, D. Gatteschi, G. Christou, and D. N. Hendrickson, J. Am. Chem. Soc. **115**, 1804 (1993).
[10] A. K. Zvezdin and A. I. Popov, JETP **82**, 1140 (1996).
[11] M. Hennion, L. Pardi, I. Mirebeau, E. Suard, R. Sessoli, and A. Caneschi, Phys. Rev. B **56**, 8819 (1997).
[12] M. I. Katsnelson, V. V. Dobrovitski, and B. N. Harmon, Phys. Rev. B **59**, 6919 (1999).
[13] A. L. Barra, D. Gatteschi, and R. Sessoli, Phys. Rev. B **56**, 8192 (1997).
[14] C. Raghu, I. Rudra, D. Sen, and S. Ramasesha, Phys. Rev. B **64**, 064419 (2001).
[15] A. Lascialfari, D. Gatteschi, F. Borsa, A. Shastri, Z. H. Jang, and P. Carretta, Phys. Rev. B **57**, 514 (1998); A. Lascialfari, Z. H. Jang, F. Borsa, P. Carretta, and D. Gatteschi, Phys. Rev. Lett. **81**, 3773 (1998).
[16] D. Arčon, J. Dolinšek, T. Apih, R. Blinc, N. S. Dalal, and R. M. Achey, Phys. Rev. B **58**, R2941 (1998).
[17] Y. Furukawa, K. Watanabe, K. Kumagai, Z. H. Jang, A. Lascialfari, F. Borsa, D. Gatteschi, Phys. Rev. B **62**, 14246 (2000).
[18] T. Goto, T. Kubo, T. Koshiba, J. Arai, Y. Fujii, A. Oyamada, K. Takeda, and K. Awaga, Physica B **284-288**, 1227 (2000).
[19] Y. Furukawa, K. Watanabe, K. Kumagai, F. Borsa, and D. Gatteschi, Phys. Rev. B **64**, 104401 (2001).
[20] R. M. Achey, P. L. Kuhns, A. P. Reyes, W. G. Moulton, and N. S. Dalal, Phys. Rev. B **64**, 064420 (2001); Solid State Commun. **121**, 107 (2002).
[21] S. Yamamoto and T. Fukui, Phys. Rev. B **57**, R14008 (1998).
[22] E. M. Chudnovsky, Science **274**, 938 (1996).
[23] R. Sessoli, D. Gatteschi, A. Caneschi, and M. A. Novak, Nature **365**, 141 (1993).
[24] M. Takahashi, Phys. Rev. Lett. **58**, 168 (1987).
[25] S. Yamamoto, T. Fukui, K. Maisinger, and U. Schollwöck, J. Phys.: Condens. Matter **10**, 11033 (1998); S. Yamamoto, T. Fukui, and T. Sakai, Eur. Phys. J. B. **15** (2000) 211.
[26] T. Nakanishi and S. Yamamoto, Phys. Rev. B **65**, June 1 (2002).
[27] T. Kubo, T. Goto, T. Koshiba, K. Takeda, and K. Awaga, submitted to Phys. Rev. B.

TABLE I. Estimates of $(g\mu_{\rm B}\gamma_{\rm N}A_i)^2$ in the unit of $({\rm rad}\cdot{\rm Hz})^2$ under the parametrizations (a) and (b) compared with experimental findings [19].

	Mn(1)	Mn(2)	Mn(3)
Parameters (a)	7.9×10^{17}	3.2×10^{18}	3.7×10^{18}
Parameters (b)	6.5×10^{16}	2.7×10^{17}	3.0×10^{17}
Experimental	1.1×10^{16}	9.3×10^{16}	2.0×10^{17}